

$\text{Bi}_{12}\text{Sr}_{22}\text{Fe}_{11}\text{O}_{56}$: A new form of 2201/0201 “terraces” like structures, term $m = 6$, $n = 11$ of the $[\text{BiO}_2]_m[\text{Sr}_2\text{FeO}_4]_n$ family

Mathieu Allix*, Denis Pelloquin, Bernard Raveau

Laboratoire CRISMAT, UMR 6508-CNRS, ISMRA et Université de Caen, 6, Boulevard du Maréchal Juin, 14050 Caen Cedex, France

Received 26 October 2004; received in revised form 17 January 2005; accepted 27 January 2005

Abstract

A new oxide, namely $\text{Bi}_{12}\text{Sr}_{22}\text{Fe}_{11}\text{O}_{56}$, has been isolated in the Bi–Sr–Fe–O system. The transmission electronic microscopy studies carried out have permitted to characterise it as a double collapsed member derived from the regular intergrowth 2201/0201 type structure $\text{Bi}_2\text{Sr}_4\text{Fe}_2\text{O}_{10}$ (J. Solid State Chem. 118 (1995) 227). It crystallises in the space group $I2/a$ with the following parameters: $a = 38.82(1)\text{Å}$, $b = 5.731(2)$, $c = 38.35(1)\text{Å}$ and $\beta = 121.31(2)^\circ$. Close relationships with the collapsed structure $\text{Bi}_{13}\text{Ba}_2\text{Sr}_{25}\text{Fe}_{13}\text{O}_{66}$ ($m = 7$, $n = 13$) are shown. This new ferrite can be described as the ($m = 6$, $n = 11$) member of the $[\text{Bi}_2\text{O}_2]_m[\text{Sr}_2\text{FeO}_4]_n$ family. The stairs are then 6 bismuth atoms wide and the K_2NiF_4 layers are 11 FeO_6 octahedra thick. Moreover, the high-resolution electron microscopy images show the presence of local defects leading to the ($m = 7$, $n = 11$) member. Another description of this structure is also considered: it can be understood as slices of the parent structure, $\text{Bi}_2\text{Sr}_4\text{Fe}_2\text{O}_{10}$, separated by shearing zones. If the last ones seem to be the same in all the members, the thickness of the first ones can vary and so leading to different members of the new $[\text{Bi}_2\text{Sr}_4\text{Fe}_2\text{O}_{10}]_w[\text{Bi}_4\text{Sr}_6\text{Fe}_3\text{O}_{16}]_v$ family.

© 2005 Elsevier Inc. All rights reserved.

Keywords: Transmission electron microscopy; Bi–Sr–Fe–O system; X-ray diffraction; Collapsed structure; Shearing phenomena; Iron; $\text{Bi}_{12}\text{Sr}_{22}\text{Fe}_{11}\text{O}_{56}$; $\text{Bi}_2\text{Sr}_4\text{Fe}_2\text{O}_{10}$

1. Introduction

The various investigations of the Bi–Sr–Fe–O system have shown its extraordinary richness. The pseudo-ternary diagram Bi_2O_3 – Fe_2O_3 – SrO (Fig. 1) exhibits indeed about eleven oxides, most of them being closely related to layered structures with very close compositions. A great number of them, such as 1201, 2201, 2212 or 2223 structures result from intergrowths of perovskite layers with distorted rock salt-type layers [1,3–13] and moreover exhibit sometimes additional cationic orderings. Besides those oxides, several layered oxides involving complex shearing mechanisms have been isolated [14–16]. The latter, so-called collapsed

structures, are based on the 2212 intergrowth $\text{Bi}_2\text{Sr}_3\text{Fe}_2\text{O}_9$ and can be deduced from this structure by applying a shearing mechanism every four or five FeO_6 octahedra, so that the 2212 slices formed are interconnected through “ $\text{Bi}_2\text{Sr}_3\text{FeO}_8$ ” blocks. In spite of the close relationships between the 2201 and 2212 structures, no collapsed structure derived from the 2201/0201 $\text{Bi}_2\text{Sr}_4\text{Fe}_2\text{O}_{10}$ oxide has been observed to date in the Bi–Sr–Fe–O system. Nevertheless, by replacing partly strontium by barium in such a stacking, a similar structural feature can be observed, leading to the oxide $\text{Bi}_{13}\text{Ba}_2\text{Sr}_{25}\text{Fe}_{13}\text{O}_{66}$ [2]. The latter has been described as stair-like Bi_2O_2 layers parallel to (001) intergrown with K_2NiF_4 -type layers. The stairs that form the bismuth oxygen layers are 7 bismuth atoms wide, whereas the K_2NiF_4 layers are 13 FeO_6 octahedra thick, so that this structure can be considered as the $m = 7$, $n = 13$ member of a series of ferrites $[\text{Bi}_{2-x}\text{Ba}_x\text{O}_2]_m[\text{Sr}_{2-x}\text{Ba}_x\text{FeO}_4]_n$.

*Corresponding author. The Department of Chemistry, The University of Liverpool, Crown Street, Liverpool L69 7ZD, UK. Fax: +44 151 794 3588.

E-mail address: allix@liverpool.ac.uk (M. Allix).

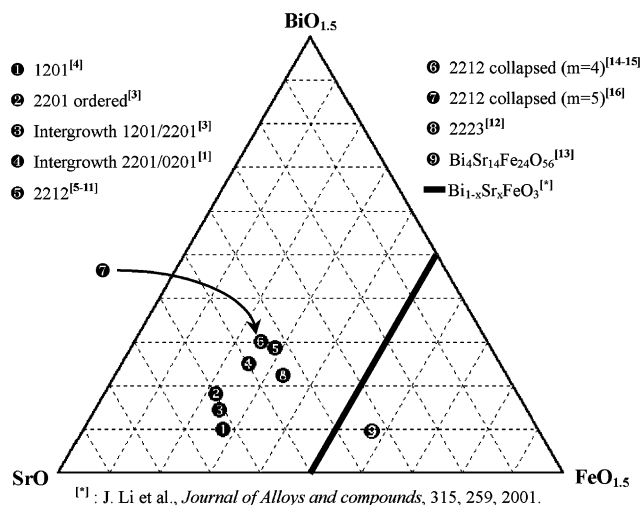


Fig. 1. Pseudo-ternary diagram of the Bi–Sr–Fe–O system.

In order to understand the role of strontium and barium cations in the stabilisation of such collapsed structures, we have revisited the Bi–Sr–Fe–O system, controlling the conditions of synthesis. The present paper reports on a new ferrite $\text{Bi}_{12}\text{Sr}_{22}\text{Fe}_{11}\text{O}_{56}$ which derives also from the 2201/0201 structure by a double collapsing mechanism, showing that barium is not necessary to induce some shearing phenomena in the $\text{Bi}_2\text{Sr}_4\text{Fe}_2\text{O}_{10}$ 2201/0201-type structure. From TEM observations, it can be described as a new member “ $m = 6, n = 11$ ” of the $[\text{Bi}_2\text{O}_2]_m[\text{Sr}_2\text{FeO}_4]_n$ family. Moreover, HREM images show that several defects are possible and define this compound as the intergrowth between 2201/0201 parent structure slices and collapsed zones, as it has been shown in the 2212 collapsed structure [16].

2. Experimental section

2.1. Chemical synthesis

$\text{Bi}_{12}\text{Sr}_{22}\text{Fe}_{11}\text{O}_{56}$ was prepared from stoichiometric amount of Bi_2O_3 , Fe, Fe_2O_3 and SrO. Each preparation was performed in dry box using SrO oxide which was freshly prepared by heating SrO_2 or $\text{Sr}(\text{OH})_2 \cdot 8\text{H}_2\text{O}$ at 1100°C . The powder, with the nominal molar ratio Bi:2 Sr:4.3 Fe:1.7 and O:9.3 was intimately ground in an agate mortar, placed in an evacuated quartz ampoule and heated up to 1000°C during 6 h, held for 24 h and cooled at room temperature at a rate of 150°C h^{-1} . Powder appears as brown colour. Attempts to grow single crystals of this new ferrite failed.

2.2. Experimental techniques

The electron diffraction (ED) study was carried out using a JEOL 200CX microscope fitted with an

eucentric goniometer ($\pm 60^\circ$) while the high-resolution electron microscopy (HREM) images were recorded with a TOPCON 002B microscope operating at 200 kV and having a point resolution of 1.8 \AA . In order to perform the electron microscopy observations, crystals were crushed in butanol, and the small flakes were deposited on a holey carbon film, supported by a copper grid. Energy dispersive spectroscopy (EDS) analyses were systematically carried out, both electron microscopes being equipped with KEVEX analysers. Typical spot size of 10 nm has been used to scan the chemical composition for each microcrystal analysed (about thirty microcrystals have been analysed). The accuracy of analyses from this statistical technique is about 5/100 for each cation value.

The X-ray powder diffraction (XRPD) data were collected at room temperature with a PHILIPS PW 1830 vertical diffractometer working with $\text{CuK}\alpha$ radiation. Data were collected by step scanning over an angular range from $4^\circ \leq 2\theta \leq 120^\circ$ by increments of $0.02^\circ(2\theta)$ and were indexed by pattern matching with the program Fullprof [17].

3. Structural analysis

3.1. Microscopy study: the “ $m = 6, n = 11$ ” member of the $[\text{Bi}_2\text{O}_2]_m[\text{Sr}_2\text{FeO}_4]_n$ series

A nearly pure brown sample is obtained from the synthesis route as above. Only the ideal 2201/0201 structural form ($m = 1, n = 2$) has been detected as impurity. The reconstruction of the reciprocal space from ED patterns evidences a monoclinic cell for the main phase with $a \approx 39 \text{ \AA}$, $b \approx 5.7 \text{ \AA}$, $c \approx 38 \text{ \AA}$ and $\beta \approx 121^\circ$. The conditions limiting the reflections, hkl : $h + k + l = 2n$, involving an I lattice and the extra condition $h0l, h = 2n$ lead us to choose the $I2/a$ space group. The [100], [010] and [001] ED patterns are given in Fig. 2. The great similarity between the [010] ED pattern of our compound and those of the other collapsed ferrites in particular with the $\text{Bi}_{13}\text{Ba}_2\text{Sr}_{25}\text{Fe}_{13}\text{O}_{66}$ compound [10] is strongly in favour of a shearing phenomenon. In order to confirm this hypothesis and to propose a structural model, a HREM study has been performed.

The [010] oriented pattern is the most useful orientation to image the layer stacking mode and the collapsed mechanism. This orientation is presented in Fig. 3 where high electron density zones appear as bright dots. Such a value of defocalisation allows correlating the bright dots to the bismuth and strontium rows whereas the iron rows are imaged as grey dots. Thus, on the edge of the crystal, one can observe quadruple rows of bright dots alternating with double ones and separated by one single row of darker spots. Such an observation can be interpreted by the following layer

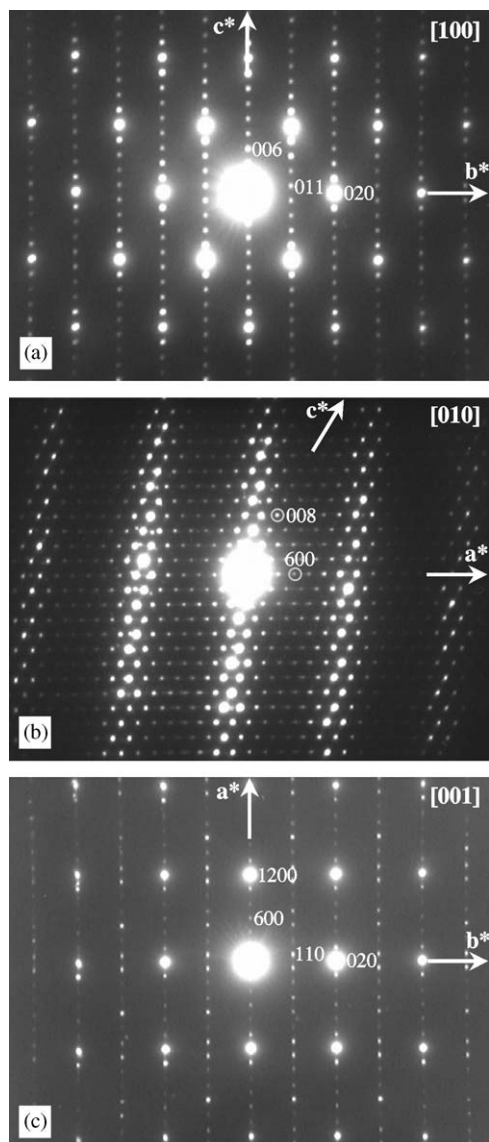
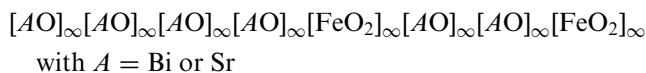


Fig. 2. Experimental ED patterns in the [100], [010] and [001] directions.

stacking mode:



in agreement with an intergrowth between one 2201 and one 0201 slices. We can notice that several intergrowth defects, correlated to extra (0201) and collapsed (2201) sequences (labeled ① and ② in Fig. 3 respectively), are also observed in the edge of the crystal.

Moreover, deeper in the crystal, a double shearing mechanism clearly appears (Fig. 3). The corresponding structural model is shown in Fig. 4. First, starting from the 2201/0201 intergrowth drawn in Fig. 4a, a shearing mechanism applied along the $c_{2201/0201}$ direction of this structure every six bismuth atoms takes place. Secondly, two successive $[AO]_{\infty}$ discontinuous

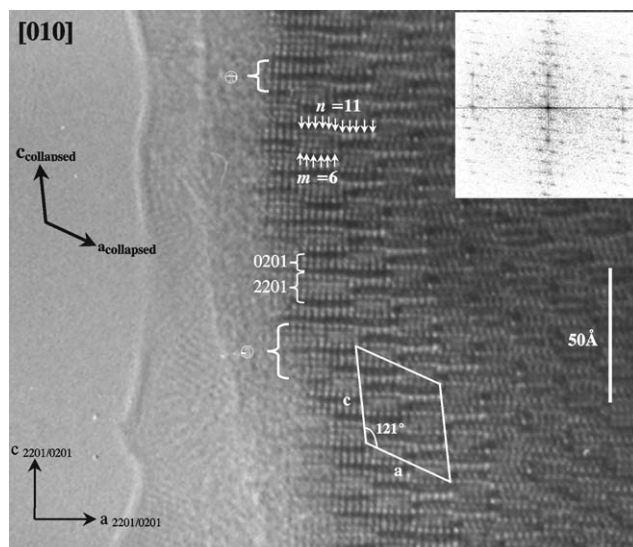


Fig. 3. Experimental HREM image recorded along the collapsed (i.e. the [010]) direction). Two defects related to (2201)/(0201) and collapsed 2201 can be observed and are labeled ① and ②, respectively. The calculated Fourier transformed of the image is shown in inset.

layers are brought closer together by a translation along $a_{2201/0201}$. This leads, by the suppression of 1 FeO_6 octahedron out of 12, to a double collapsed structure (Fig. 4b). The latter leads to the theoretical formula $\text{Bi}_{12}\text{Sr}_{22}\text{Fe}_{11}\text{O}_{56}$ or $\text{Bi}_{2.13}\text{Sr}_{3.91}\text{Fe}_{1.96}\text{O}_{9.96}$ by referring to the ideal 2201/0201-parent structure $\text{Bi}_2\text{Sr}_4\text{Fe}_2\text{O}_{10}$.

By considering now the EDS analyses performed on many crystals, the average cationic composition is $\text{Bi}_{11.9}\text{Sr}_{22.5}\text{Fe}_{10.6}$. This composition is very close to the expected one $\text{Bi}_{12}\text{Sr}_{22}\text{Fe}_{11}$. Several cells can be considered, but in agreement with the previous studies on similar structures [9,10], we have chosen a cell with a β value close to 120° . Thus, the cell parameters have been refined in monoclinic $I2/a$ symmetry from X-ray diffraction patterns (Fig. 5) to the following values:

$$a = 38.82(1)\text{\AA}, \quad b = 5.731(2)\text{\AA}, \quad c = 38.35(1)\text{\AA}$$

and $\beta = 121.31(2)^\circ$.

Thus, according to this HREM study, the $\text{Bi}_{12}\text{Sr}_{22}\text{Fe}_{11}\text{O}_{56}$ oxide can be described as the $m = 6, n = 11$ member of the $[\text{Bi}_2\text{O}_2]_m[\text{Sr}_2\text{FeO}_4]_n$ family. The volume of the corresponding cell and the numerous defects detected during these HREM observations (shown in Figs. 3 and 6) do not allow performing structural refinements from powder X-ray diffraction data. A realistic structural study of this complex modulated structure can be only carried out from single crystal data.

3.2. Evidence for extended defects along a-axis: premises of new members

The shearing mechanism described above is made complicated by the appearance of numerous extended

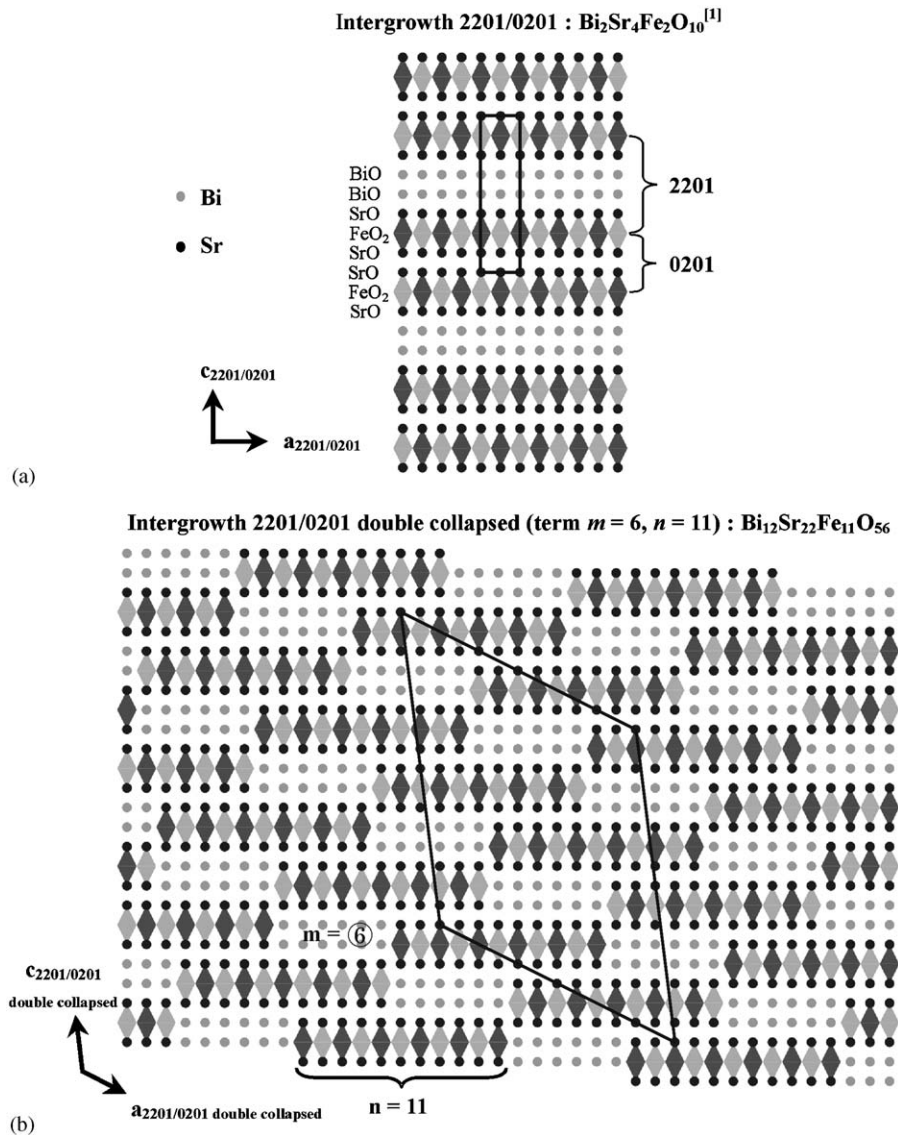


Fig. 4. Schematic structures projected along b of: (a) the $\text{Bi}_2\text{Sr}_4\text{Fe}_2\text{O}_{10}$ original 2201/0201 intergrowth and (b) the double collapsed $\text{Bi}_2\text{Sr}_4\text{Fe}_2\text{O}_{10}$ structure.

defects. The most common one consists in the variation of the width of the BiO tapes. Sometimes, instead of being six atoms wide, they can be seven Bi atoms wide. This is illustrated by the HREM image shown in Fig. 6. Indeed, one can always see the same collapsing mechanism leading to the structure previously described, but by looking carefully at the level of the width of the BiO tapes, one can count seven bright dots, correlated to the Bi atoms along the $a_{2201/0201}$ direction. This leads to consider a $m = 7$ local member. But considering now the n value, one still observes a $n = 11$ value. This feature can be explained by the fact that a bismuth atom takes locally the place of an iron one, as proposed on the model in Fig. 7. In the latter, at the level of the dotted circle the position is occupied by

an iron atom in the case of the $m = 6$ member and by a Bi atom in the case of the $m = 7$ member. This explanation, coming from the contrast of the HREM images agrees with a non-variation of the n value. A similar variation of the width of BiO tapes has already been observed in the case of the $\text{Bi}_{13}\text{Ba}_2\text{Sr}_{25}\text{Fe}_{13}\text{O}_{66}$ [10] compound.

4. Discussion and conclusion

Inspired by the work on the 2212 collapsed structures previously reported [14–16], we propose now to compare the two structural models of $\text{Bi}_{13}\text{Ba}_2\text{Sr}_{25}\text{Fe}_{13}\text{O}_{66}$ and $\text{Bi}_{12}\text{Sr}_{22}\text{Fe}_{11}\text{O}_{56}$ oxides (Fig. 8). A new

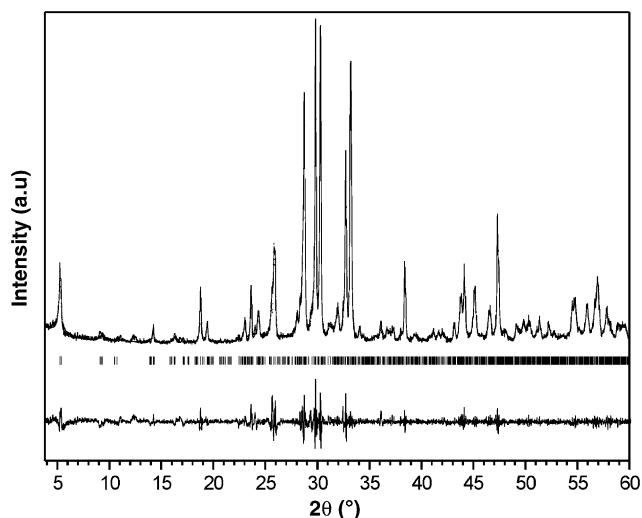


Fig. 5. Representation of the Le Bail fit carried on powder X-ray pattern of $\text{Bi}_{12}\text{Sr}_{22}\text{Fe}_{11}\text{O}_{56}$.

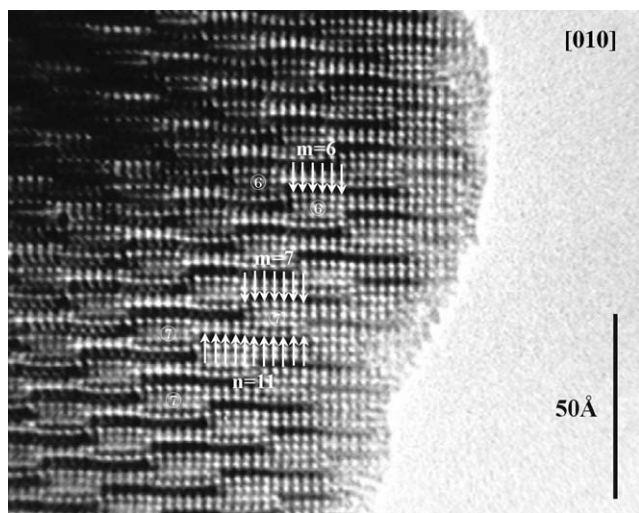


Fig. 6. Experimental HREM image recorded along the [010] direction showing the presence of $m = 7, n = 11$ defects.

description for this family can thus be proposed. Effectively, by considering the collapsed structures as composed of $2201/0201$ slices and shearing zones, the arrangement of such structures is more understandable. This modelling corresponds to an intergrowth between $2201/0201$ slices of variable thickness with a composition $[\text{Bi}_2\text{Sr}_4\text{Fe}_2\text{O}_{10}]_w$ which alternate with invariable intermediate shearing zones of $[\text{Bi}_4\text{Sr}_6\text{Fe}_3\text{O}_{16}]$ composition. Such a description leads then to describe these two oxides as, respectively, the $w = 5$ and $w = 4$ members of the theoretical $[\text{Bi}_2\text{Sr}_4\text{Fe}_2\text{O}_{10}]_w$, $[\text{Bi}_4\text{Sr}_6\text{Fe}_3\text{O}_{16}]$ family. Taking into account the possible cationic substitutions at the level of shearing zone as reported in the previous single crystals studies of the $m = 4, 5$ members of

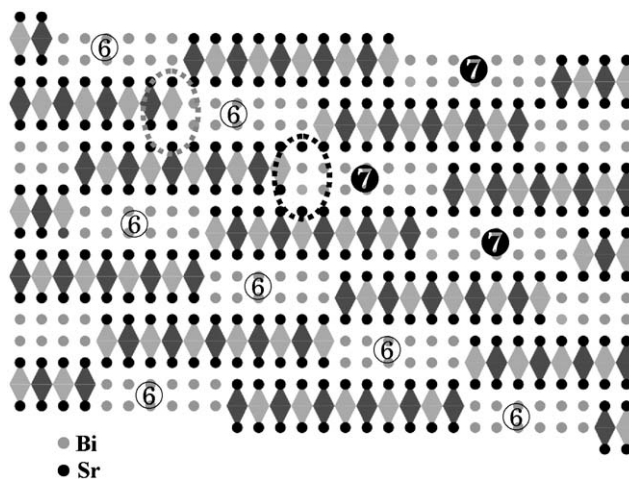


Fig. 7. Schematic structure of the $m = 7, n = 11$ member.

the $[\text{Bi}_2\text{Sr}_3\text{Fe}_2\text{O}_9]_m[\text{Bi}_4\text{Sr}_6\text{Fe}_2\text{O}_{16}]_n$ - 2212 type collapsed family [14–16], the analysis of these peculiar zones evidences a great analogy between both series.

Otherwise, in order to better understand the formation of the collapsed structure, it is interesting to focus on the experimental conditions of synthesis. In the case of $\text{Bi}_{13}\text{Ba}_2\text{Sr}_{25}\text{Fe}_{13}\text{O}_{66}$, the possibility to induce double shearing phenomena in the $\text{Bi}_2\text{Sr}_4\text{Fe}_2\text{O}_{10}$ structure can be explained by the presence of barium, which exhibits a larger size compared to strontium. Such a reason cannot be invoked for $\text{Bi}_{12}\text{Sr}_{22}\text{Fe}_{11}\text{O}_{56}$, so that the composition, i.e. the bismuth and especially the oxygen contents, may have an important role in the appearance of shearing phenomena. In this respect, the synthesis conditions of the collapsed $\text{Bi}_{13}\text{Ba}_2\text{Sr}_{25}\text{Fe}_{13}\text{O}_{66}$ [2] and $\text{Bi}_{12}\text{Sr}_{22}\text{Fe}_{11}\text{O}_{56}$ ferrites, prepared under nitrogen flow and in sealed tube, respectively, in contrast to the parent structure $\text{Bi}_2\text{Sr}_4\text{Fe}_2\text{O}_{10}$ synthesised in air [1], may have determinant influence. The best way to clarify this point will be to isolate these different members in the same synthesis conditions.

In conclusion, a new member ($m = 6, n = 11$) of the double collapsed structure $[\text{Bi}_2\text{O}_2]_m[\text{Sr}_2\text{FeO}_4]_n$ family has been synthesised. This result shows that the presence of barium is not necessary to induce these shearing phenomena and suggests that by controlling the synthesis conditions like the nominal oxygen stoichiometry carefully, it should be possible to stabilise the other members of the series. Further experimental investigations, like the choice of starting oxides and the growth of single crystals, will be necessary to understand the role of oxygen and bismuth nonstoichiometry in the formation of these phases. This work will allow to define the shearing zones and to base the occurrence of these complex structures comparing simulated images with the experimental HREM images recorded for these collapsed $2201/0201$ structures.

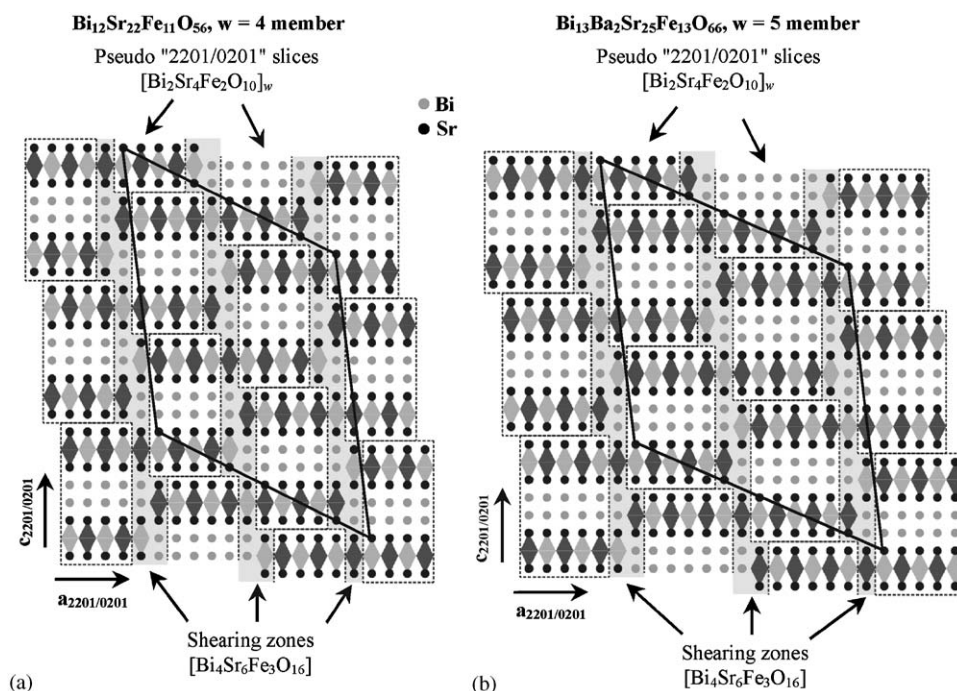


Fig. 8. Schematic structure of the $n = 11$ and $n = 13$ collapsed structures corresponding to the $w = 4$ and $w = 5$ members of the generic $[\text{Bi}_2\text{Sr}_4\text{Fe}_2\text{O}_{10}]_w$ $[\text{Bi}_4\text{Sr}_6\text{Fe}_3\text{O}_{16}]$ family.

Acknowledgments

The authors thank to Prof. M. Hervieu for the fruitful discussions and the Regional Council of Basse-Normandie for its financial support.

References

- [1] M. Hervieu, D. Pelloquin, C. Michel, M.T. Caldes, B. Raveau, *J. Solid State Chem.* 118 (1995) 227.
- [2] M. Hervieu, M.T. Caldes, C. Michel, D. Pelloquin, B. Raveau, *J. Solid State Chem.* 118 (1995) 357.
- [3] D. Pelloquin, M. Allix, C. Michel, M. Hervieu, B. Raveau, *Philos. Mag. B* 81 (11) (2001) 1669–1685.
- [4] M. Allix, D. Pelloquin, F. Studer, N. Nguyen, A. Wahl, A. Maignan, B. Raveau, *J. Solid State Chem.* 167 (2002) 48.
- [5] M. Hervieu, C. Michel, N. Nguyen, R. Retoux, B. Raveau, *Eur. J. Solid State Inorg. Chem.* 25 (1988) 375.
- [6] O. Perez, H. Leligny, D. Grebille, P. Labbe, D. Groult, B. Raveau, *J. Phys.: Condens. Matter* 7 (1995) 10003; O. Perez, H. Leligny, D. Grebille, J.M. Grenèche, P. Labbe, D. Groult, B. Raveau, *Phys. Rev. B* 55 (1997) 1236.
- [7] G. Mayer-Von Kürty, T. Fries, A. Ehmann, S. Kemmler-Sack, *J. Less-Common Met.* 155 (1989) L19.
- [8] Y. Lepage, W.R. Mckinnon, J.M. Tarascon, P. Barboux, *Phys. Rev. B* 40 (1989) 6810.
- [9] T. Fries, C. Stuedtner, M. Schlichenmaier, S. Kemmler-Sack, T. Nissel, R.P. Huebener, *J. Solid State Chem.* 109 (1994) 88.
- [10] D. Hechel, I. Felner, *Physica B* 262 (1999) 410.
- [11] V. Sedykh, I. Smirnova, B. Bagautdinov, K. Hagiya, M. Ohmasa, E. Suvorov, A. Dubovitskii, V. Shekhtman, *Physica C* 355 (2001) 87.
- [12] R. Retoux, C. Michel, M. Hervieu, N. Nguyen, B. Raveau, *Solid State Commun.* 69 (1989) 599.
- [13] C. Lepoitevin, S. Malo, D. Grebille, M. Hervieu, B. Raveau, *Chem. Mater.* 16 (2004) 5731.
- [14] M. Hervieu, O. Perez, D. Groult, D. Grebille, H. Leligny, B. Raveau, *J. Solid State Chem.* 129 (1997) 214.
- [15] O. Perez, H. Leligny, G. Baldinozzi, D. Grebille, M. Hervieu, P. Labbe, D. Groult, *Phys. Rev. B* 56 (1997) 5662.
- [16] M. Allix, O. Perez, D. Pelloquin, M. Hervieu, B. Raveau, *J. Solid State Chem.* 177 (2004) 3187.
- [17] J. Rodriguez-Carvajal, Proceedings of the Satellite Meeting on Powder Diffraction of the XVth Congress of the International Union of Crystallography, Toulouse, France, 1990.